Int. J. Heat Mass Transfer. Vol. 32, No. 1, pp. 131–145, 1989
Printed in Great Britain

0017-9310/89 $3.00 + 0.00
© 1989 Pergamon Press plc

Horizontal flow boiling heat transfer experiments with a mixture of R22/R114

D. S. JUNG,† M. McLINDEN,‡ R. RADERMACHER† and D. DIDION‡

† Department of Mechanical Engineering, University of Maryland, College Park, MD 20742, U.S.A.
‡ Thermal Machinery Group, National Bureau of Standards, Gaithersburg, MD 20899, U.S.A.

(*Received* 8 *January* 1988 *and in final form* 24 *May* 1988)

Abstract—An experimental study on horizontal flow boiling heat transfer for pure R22, R114 and their mixtures under uniform heat flux condition is reported. More than 1200 local heat transfer coefficients are obtained for annular flow at a reduced pressure of 0.08. The ranges of heat flux and mass flow rate are 10–45 kW m^{-2} and 16–46 g s^{-1}, respectively. The results indicate a full suppression of nucleate boiling for pure and mixed refrigerants beyond transition qualities and the majority of the data belongs to the convective evaporation region. The heat transfer coefficients of mixtures in this region are as much as 36% lower than the ideal values under the same flow condition. Non-ideal variations in physical properties account for 80% of the heat transfer degradation seen with mixtures and the other 20% (less than 10% of the heat transfer coefficient) is believed to be caused by mass transfer resistance in this region. A composition variation of up to 0.07 mole fraction in the annular liquid film was measured between the top and bottom of the tube, which causes a corresponding circumferential variation of wall temperature with mixtures.

1. INTRODUCTION

IT HAS been shown in earlier studies [1–3] that non-azeotropic refrigerant mixtures increase the coefficient of performance of heat pumps emphasizing energy conservation. One of the characteristics of non-azeotropic mixtures is the variable temperature during phase change at constant pressure. This phenomenon can be utilized to reduce the thermodynamic irreversibility in counter-current heat exchangers resulting in an increase in heat exchanger efficiency.

Studies in an experimental heat pump using non-azeotropic refrigerant mixtures as working fluids have demonstrated an increase in the coefficient of performance of up to 32% for an optimized mixed refrigerant as compared to the performance with R22 [1]. In addition, mixtures offer numerous other advantages such as capacity control and lower pressure ratios across the compressor [2, 3]. In spite of these advantages, however, the use of refrigerant mixtures in heat pumps has not yet been popular due in part to the lack of such information as heat transfer coefficients. Of particular concern in this paper is the horizontal flow boiling heat transfer characteristics of a non-azeotropic refrigerant mixture during evaporation.

Two-phase flow boiling heat transfer has been the subject of extensive research for the past few decades. In particular, much work has been carried out with water in vertical channels with applications in nuclear and conventional power plants. In contrast to the geometry and low quality range in power plant applications, evaporator coils in heat pumps are usually horizontal and the quality range of interest is typically 20–100%. While there are many studies reported in the literature regarding the flow boiling heat transfer for pure refrigerants, only a few exist for refrigerant mixtures in horizontal flow.

Singal *et al.* [4] carried out experiments with an R13/R12 mixture. Their test section consisted of two identical horizontal stainless steel tubes (2.35 m long, 0.95 cm i.d.) which were heated by passing an alternating current directly through the tube. The composition of R13 in R12 was 0–20% by mass in intervals of 5%. They observed that average heat transfer coefficients for the binary mixture were slightly greater than those for pure R12. They, however, did not perform experiments with pure R13.

In ref. [5] experiments were performed with an R13B1/R152a mixture. The test section used was a 2.7 m long, 0.9 cm i.d. stainless steel tube heated by passing a direct current through it. To the contrary of the findings of Singal *et al.* [4], it was observed that local and average heat transfer coefficients for mixtures were significantly lower than those for either pure component. The results were compared with the available correlations and it was concluded that the local heat transfer correlations for pure fluids did not adequately predict the heat transfer for non-azeotropic mixtures.

As a follow on to this work, a series of experiments were conducted with an R13B1/R152a mixture having overall compositions of 0.07, 0.22, 0.36, and 0.64 mole fraction R13B1 [6]. The test section and heating method used were the same as in ref. [5] except that the test section was composed of two portions: a 2 m long preheating test section and a 0.7 m long main test section. By using a high heat flux in the preheating section, qualities available in the main test section could be made higher than those of ref. [5]. The results

NOMENCLATURE

A	heat transfer area [m^2]
C	composition
C_p	specific heat [$kJ\,kg^{-1}\,K^{-1}$]
d	internal diameter of the tube [m]
EOS	equation of state in Table 2
F	heat transfer enhancement factor in Chen's equation
fn	function in equation (14)
G	mass flux [$kg\,m^{-2}\,s^{-1}$]
HTC	heat transfer coefficient in Table 2
h	heat transfer coefficient [$W\,m^{-2}\,K^{-1}$]
h_{fg}	latent heat of vaporization [$kJ\,kg^{-1}$]
k	thermal conductivity [$W\,m^{-1}\,K^{-1}$]
$\dot{m}$	mass flow rate [$g\,s^{-1}$]
p_r	reduced pressure
Q	heat input [W]
q	heat flux [$W\,m^{-2}$]
S	suppression factor in Chen's equation
T	temperature [°C or K]
X_{tt}	Martinelli parameter, equation (7)
x	thermodynamic equilibrium quality based on mass.

Greek symbols

μ	viscosity [Pa s]
ρ	density [$kg\,m^{-3}$]
σ	surface tension [$N\,m^{-1}$]
ϕ	property and quality combination in equation (10).

Subscripts

av	average
b	bottom
cal	calculated
cec	convective evaporation contribution
eq	equilibrium
eqa	average equilibrium
eql	local equilibrium
f	fluid
g	gliding
l	liquid
lo	liquid only
ls	left-hand side
nb	nucleate boiling
nbc	nucleate boiling contribution
o	overall
rs	right-hand side
s	side
sat	saturation
t	top
tp	two phase
v	vapor
w	wall.

also showed a substantial degradation of heat transfer coefficients with an R13B1/R152a mixture.

Besides this, Ross *et al.* [6] reported for the first time a circumferential variation of wall temperatures with mixtures in an annular flow regime. In annular flow, heat is conducted across the liquid layer and especially in a horizontal geometry the liquid film at the bottom is thicker than that at the top due to gravity. Consequently, for pure components the wall temperature at the bottom of the tube was higher than that at the top because of the increased resistance to conduction heat transfer, which results in a lower heat transfer coefficient at the bottom than at the top of the heated tube. For mixtures, however, a new phenomenon, contrary to pure components' behavior, was observed: the wall temperature at the bottom was lower than the one at the top. Ross *et al.* [6] conjectured that the cause for this phenomenon might be a composition variation around the circumference of the heated tube.

Finally, data by Ross *et al.* also indicated that heat transfer coefficients for mixtures were more or less constant over the overall composition range of 0.1–0.64 mole fraction R13B1. This last observation raises the question of whether heat transfer coefficients for mixtures might be independent of composition.

From the literature review, it becomes clear that the following issues need to be resolved.

(1) What are the main reasons for the degradation of heat transfer with mixtures?

(2) Is the circumferential variation of the wall temperature for mixtures due to the composition variation?

(3) How do the heat transfer coefficients for mixtures behave at compositions close to either pure component?

As a continuation of the work carried out in refs. [5, 6], the present study was undertaken to resolve the above issues. The R22/R114 mixture, which is non-azeotropic, was selected as the working fluid because of its wide variation in boiling points (52°C at 330 kPa). Figure 1 shows the temperature–composition diagram for this mixture at 330 kPa. In this study, composition is defined as the mole fraction of the more volatile component, R22, unless otherwise specified. The bubble and dew lines divide the diagram into three regions. The bubble line represents the saturated liquid line below which the liquid is subcooled. The dew line represents the saturated vapor line above which the vapor is superheated. Between the lines is the liquid–vapor region where a mixture exists in two phases.

When a binary non-azeotropic mixture undergoes evaporation or condensation, the compositions of the two components are different in the vapor and liquid

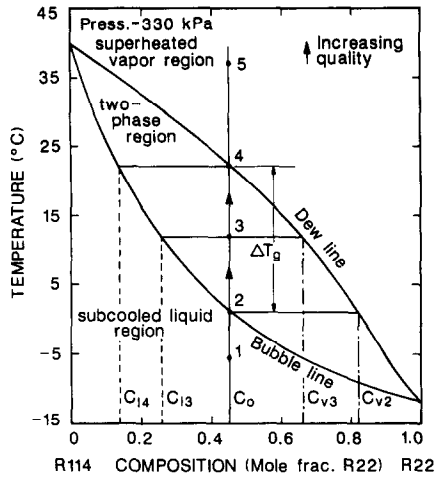

FIG. 1. Temperature–composition diagram for R22/R114 mixture at 330 kPa.

phases. This can be illustrated by describing the evaporation process of an R22/R114 mixture in Fig. 1. For a given overall composition, C_o, a liquid phase alone exists with a composition of $C_{l1} = C_o$ at state 1. State 2 is on the saturated liquid line and has a liquid phase composition of $C_{l2} = C_o$ in equilibrium with a vapor of composition C_{v2}. As the evaporation process continues to state 3, the composition shifts to C_{l3} for the liquid phase and C_{v3} for the vapor phase. Reaching the saturated vapor curve at state 4 gives a liquid composition of C_{l4} and vapor composition $C_{v4} = C_o$. Further heating evaporates all the liquid so that at state 5 a superheated vapor exists at $C_{v5} = C_o$.

There are several observations to make from this diagram during evaporation of mixtures. As quality is increased, the liquid phase becomes richer in the less volatile component while the vapor phase is richer in the more volatile component. In addition, the evaporation process at a constant pressure does not occur at a constant temperature but rather over a range of temperatures, referred to as the gliding temperature effect (represented as ΔT_g in Fig. 1). For a fixed overall composition, as quality increases, so does the equilibrium temperature, T_{eq}. This refrigerant pair also reveals large composition differences of as much as 0.4 mole fraction between the liquid and vapor phases, which is expected to exert a strong mixture effect known as the mass transfer resistance on nucleate boiling heat transfer as shown by Stephan [7].

2. EXPERIMENTS

2.1. *Experimental apparatus*

In order to avoid a thermal entry length effect on heat transfer coefficient due to a short test section [8] and achieve high exit quality even at low heat fluxes, a long test section was constructed for the present study. A schematic view of the experimental apparatus is given in Fig. 2. The test section was made of two 4 m long by 0.9 cm i.d. stainless steel tubes with a wall thickness of 0.25 mm. These two sections were 0.5 m apart and connected by a 180° U-turn bend.

There are three bus connections to the d.c. power supply on the first 4 m section and five on the second 4 m section. These bus connections effectively created a variable length test section, which was one of the distinctive features of the current rig. For instance, for high heat flux and low mass flow rate, only a part of the 8 m test section was heated to give an exit quality of 70–80%. For low heat flux and high mass flow rate, however, the full 8 m test section was heated to achieve a reasonably high exit quality.

The flow loop is described as follows; a semi-hermetic, oil-free pump delivers a subcooled liquid to the test section. Just before the test section inlet, a calibrated turbine flow meter and a flow regulating valve are installed to measure and control the flow rate. The subcooled liquid is heated by passing a d.c. current through the tube supplied by a low voltage (0–60 V), high current (0–300 A) power supply. The vapor generated in the test section is condensed in the condenser which is cooled by brine at -20 to -60°C. The pump then draws the liquid from the bottom of the condenser to complete the cycle. The flow patterns were observed through the sight glasses installed before and after the test section. All tests were run with a subcooled liquid entering the test section. In order to reduce the heat gain (or loss) from (or to) the surroundings, the test section was covered with fiber glass insulation 20 cm in diameter.

Instream refrigerant temperatures, needed for energy balance analysis, were measured at the inlet, outlet, and before and after the U-turn bend by stainless steel-sheathed, isolated thermocouples. The outside wall temperatures on the heated tube were measured by 30 gage copper–constantan thermocouples mounted in 17 stations. Each station had four thermocouples which were clamped on the top, bottom, and both sides of the tube. They were electrically insulated from the tube by a thin layer of PTFE (teflon) tape. All thermocouples were referenced to a refrigerated ice bath. Static pressure taps were manufactured on each bus connection by electrical discharge machining. Four calibrated pressure transducers and one differential pressure transducer in conjunction with two 5-way valves were used to measure the static pressures at the eight pressure taps and the pressure drops across various segments of the test section.

2.2. *Data collection, reduction, and analysis*

All tests were run at steady-state conditions. Data acquisition and control of the system were carried out by a data logger and a microcomputer. The data acquisition system continuously scanned and stored all inputs while the system was coming to steady state which was indicated by monitoring several key system temperatures and also the sum of the differences between successive scans of all the recorded variables. A single scan took 90 s to record 89 e.m.f. values from

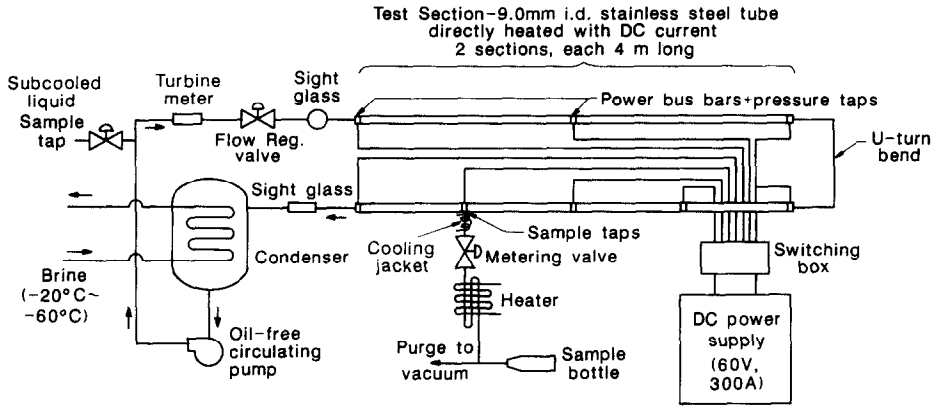

FIG. 2. Schematic view of experimental apparatus.

thermocouples, 8 d.c. voltages from the bus connections, 1 d.c. voltage from the standard resistor (for the measurement of current on the test section), 9 voltages from the pressure transducers, and 1 frequency reading from the turbine flow meter. It usually took 1–2 h for the system to reach steady state. When steady-state conditions were observed for more than 20 scans, these scans were stored and constituted a test.

For each mixture test, a liquid sample was drawn immediately after a test from the subcooled liquid line before the turbine meter as shown in Fig. 2 and this was analyzed by gas chromatography to give the overall composition of the working fluid entering the test section. This overall composition differed from the initially charged composition by 2–3% in mole fraction depending upon how much vapor was generated in the system. The vapor generated is enriched in a more volatile component, which results in a composition shift of the remaining liquid to a less volatile component due to species balance requirement. This fact defies the assumption made by Singal *et al.* [4] that the overall composition of the liquid entering the test section is the same as the initially charged composition throughout the tests.

In order to determine the local heat transfer coefficients from these data, the following equation was employed:

$$Q = hA(T_w - T_f). \quad (1)$$

The inner wall temperatures, T_w, were calculated from the measured outside wall temperatures by the one-dimensional, radial, steady-state heat conduction equation assuming uniform heat generation within the tube wall and an adiabatic condition on the outside of the tube. The corrections made by this procedure were usually 0.1–0.3°C.

The fluid temperatures, T_f, were calculated rather than directly measured because of the difficulty of installing an instream thermocouple at each wall thermocouple station but more importantly because of the large effect of instream sensors on the heat transfer [6]. For this purpose, the pressures at each thermocouple station were interpolated linearly from the measured pressures at each pressure tap. For pure components, the thermodynamic equilibrium temperature (i.e. the saturation temperature) corresponding to the interpolated pressure was used as a T_f in equation (1) at each thermocouple station.

For mixtures, however, the thermodynamic equilibrium temperature, T_{eq}, is a function of quality as well as pressure. At each thermocouple station, a pressure, a specific enthalpy (calculated by an energy balance from the inlet to the thermocouple station), and an overall composition, C_o, were known. The equilibrium temperatures, quality, and liquid and vapor phase compositions were calculated by the Carhahan–Starling–DeSantis (CSD) equation of state developed for refrigerant mixtures [9]. The thermodynamic equilibrium temperature thus calculated for pure and mixed refrigerants is 'averaged' meaning that this is the same for a given cross-section of the heated tube.

The measurement of wall superheat, $T_w - T_f$ in equation (1), to high accuracy puts severe requirements on the measurements of local pressure, mass flow rate, and overall composition. For pure components, the accuracy of the wall superheat depended largely upon the accuracies of the local pressure measurements (typically 3–4 kPa, corresponding to 0.3–0.4°C in saturation temperature), wall temperature measurements (0.2°C), and the CSD equation of state (0.2°C). For mixtures, besides the uncertainties in the local pressure and wall temperature measurements, the errors in the wall superheat are due to the uncertainties involved in the overall composition measurements (0.5%, corresponding to 0.3°C in saturation temperature), mass flow rate measurements for the energy balance (1%, corresponding to 0.1–0.2°C in saturation temperature), and finally due to the inaccuracy of the CSD equation of state (0.4°C).

From these uncertainties, the most probable errors in the wall superheat are estimated to be 0.35, 0.4, and 0.67°C for R22, R114, and mixtures, respectively. With these most probable errors in the wall superheat and 1.5% accuracy in heat flux, the accuracies of the

local heat transfer coefficients in equation (1) are determined to be 5–11%, 5–7%, and 5–10% for R22, R114, and mixtures, respectively, for the quality range 30–70%. Larger errors occur at high qualities due to the smaller values of wall superheat, which are typically 3, 5, and 6°C at 70% quality.

At each thermocouple station, the average local two-phase flow heat transfer coefficient, h_{tp}, was determined by

$$h_{tp} = (h_t + h_{ls} + h_{rs} + h_b)/4. \quad (2)$$

2.3. *Local liquid film composition measurements*

In order to resolve the issue of whether the circumferential wall temperature variation seen with mixtures is due to a corresponding circumferential composition variation, local liquid film compositions were measured by drawing samples from the thin liquid annulus. Three sampling taps were made on the top, side, and bottom of the tube through the bus connection located 7 m from the inlet as shown in Fig. 2. Fine holes (<0.5 mm) were prepared on the tube by electrical discharge machining (spark erosion) to ensure a smooth, burr-free inner surface. Double pattern fine metering valves were used to control the sampling flow rate.

Since the liquid may flash to vapor before reaching the valve and thus affect the flow rate, the valve and the sample lines upstream of the valve were completely wrapped by a cooling jacket to insure that only subcooled liquid entered the valve. After passing through the metering valve, the liquid was heated to a superheated vapor. For each run, the sample lines were purged to a vacuum for 10–20 min. Samples from the top, side, and bottom of the tube were then simultaneously collected in evacuated sample bottles for later composition analysis by gas chromatography.

The difficulty of the measurements arises from the fact that only liquid is to be sampled since the composition of the vapor flowing in the core of the tube is quite different from that for the liquid film in the two-phase region. A variety of valve settings were tried initially until further decrease in the valve opening resulted in no change in composition indicating that only liquid was sampled. Flow rates through the valve were estimated by measuring the rate of pressure increase in the sampling bottle and they were always below 0.25 ml min^{-1} of liquid.

2.4. *Data verification*

In order to check the reliability of the current test facility, several single phase heated tests were performed for pure and mixed refrigerants and the results were compared to the well-known Dittus–Boelter equation

$$h_l = 0.023 \frac{k_l}{d} \left(\frac{Gd}{\mu_l}\right)^{0.8} \left(\frac{C_{pl}\mu_l}{k_l}\right)^{0.4}. \quad (3)$$

All single phase heated data were found to be in good agreement within an average deviation of 7% from equation (3). For each of these runs, an energy balance analysis was performed for the entire loop. The energy gained by the refrigerant across the entire test section was calculated by measured instream fluid temperatures, mass flow rate, and specific heat of the fluid. This was compared to the sum of the power input and heat gain from the surroundings. For all single phase heated tests, this energy balance was satisfied within 7%.

3. RESULTS AND DISCUSSION

A series of tests were carried out for pure and mixed refrigerants of R22 and R114 at several overall compositions. The ranges of heat flux and mass flow rate considered for this study were 10, 17, 26, 36, and 45 kW m^{-2} and 16, 23, 33, and 46 g s^{-1} (corresponding to 250–720 kg m^{-2} s^{-1} in terms of mass flux). These ranges are typical in heat pump applications. In order to avoid physical burnout of the test section, qualities at the outlet of the test section were adjusted not to exceed 85–90%, which was based on Chaddock and Mathur's observations [10].

In order to compare the results on the same basis, the pressure at the outlet of the test section was kept at a reduced pressure of 0.08, which corresponds to 400 and 260 kPa for pure R22 and R114, respectively. The reason for setting the test condition at the same reduced pressure is based on the recent studies done by Soumerai [11] and Cooper [12]. Soumerai showed that a generalized method based on a reduced pressure is particularly useful in refrigeration evaporator design optimization. Cooper also employed the same principle of corresponding states to correlate nucleate boiling heat transfer data with a simple equation having reduced pressure as one of the main variables. The reduced pressures for mixtures were determined from critical pressures calculated by a linear mole fraction weighting (ideal mixing rule) of the pure component critical pressure values. Due to pressure drops, however, pressures along the test section were up to 20% higher than that of the outlet.

For the analysis of the data and comparison with the predictive methods, thermodynamic properties for both pure and mixed refrigerants were calculated by the CSD equation of state [9]. Transport properties for pure refrigerants were taken from NEL data [13]. For the calculation of transport properties of the mixtures, the methods described by Reid *et al.* [14] were adopted. Table 1 lists some of the physical properties for pure R22 and R114 at a reduced pressure of 0.08.

3.1. *Suppression of nucleate boiling*

Figures 3 and 4 illustrate heat transfer coefficients for pure R22 and the 47% R22/53% R114 mixture. In these figures, heat transfer coefficients are plotted as a function of quality for different mass flow rates and heat fluxes. For both pure and mixed refrigerants, heat transfer coefficients for qualities less than 20–30% are functions of heat flux indicating the existence

Table 1. Physical properties of pure R22 and R114 at a reduced pressure of 0.08

Property	Unit	R22	R114
Molecular weight	kg kmol^{-1}	86.47	170.92
Pressure	kPa	400	260
Saturated temperature	°C	−6.47	31.25
Liquid density	kg m^{-3}	1304	1435
Vapor density	kg m^{-3}	17.1	19.3
Liquid specific heat	J kg^{-1} °C^{-1}	1155	1003
Heat of evaporation	J kg^{-1}	211 000	124 100
Liquid thermal conductivity	W m^{-1} °C^{-1}	0.101	0.0626
Liquid viscosity	Pa s	2.32×10^{-4}	3.36×10^{-4}
Vapor viscosity	Pa s	1.17×10^{-5}	1.19×10^{-5}
Surface tension	N m^{-1}	0.0128	0.01
Prandtl number		2.66	5.38

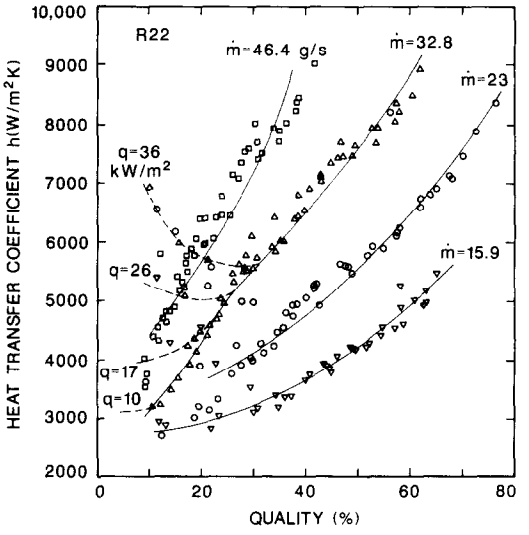

FIG. 3. Flow boiling heat transfer results for pure R22 at $p_r = 0.08$ as a function of quality for various mass flow rates. Heat flux dependence at low qualities is shown only for $\dot{m} = 32.8$ g s^{-1} as an example.

of nucleate boiling. This dependence is emphasized by the dotted lines in Figs. 3 and 4 for the flow rate of 32 g s^{-1} but is present at all other flow rates considered.

In this 'partial boiling' region, both the forced convective and nucleate boiling mechanisms are significant. The gradual suppression of the latter leads to a temporary reduction of the heat transfer coefficients with increasing quality, which was observed also in refs. [5, 6, 15]. The transition point from the partial boiling to the two-phase convective region is shown to be a function of heat flux such that it moves to a higher quality as heat flux increases for a given mass flow rate. Beyond this transition quality, however, the lines for the various heat fluxes merge into a single line indicating that nucleate boiling is suppressed.

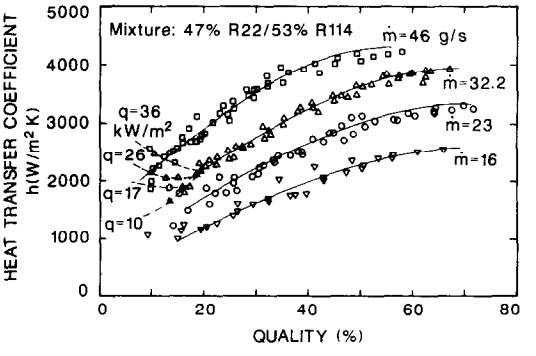

FIG. 4. Flow boiling heat transfer results for 47% R22/53% R114 at $p_r = 0.08$ as a function of quality for various mass flow rates. Heat flux dependence at low qualities is shown only for $\dot{m} = 32.8$ g s^{-1} as an example.

An earlier correlation work for two-phase saturated flow boiling heat transfer, still widely quoted, was that of Chen [16]. He divided the two-phase flow boiling heat transfer into two parts: a nucleate boiling contribution, h_{nbc}, and a convective evaporation contribution, h_{cec}, which is represented as

$$h_{tp} = h_{nbc} + h_{cec} = Sh_{nb} + Fh_{lo}. \quad (4)$$

When nucleate boiling is fully suppressed, the 'S' factor in equation (4) can be set to zero, which results in

$$\frac{h_{tp}}{h_{lo}} = F(X_{tt}) \quad (5)$$

$$h_{lo} = 0.023\frac{k_l}{d}\left(\frac{G(1-x)d}{\mu_l}\right)^{0.8}\left(\frac{C_{pl}\mu_l}{k_l}\right)^{0.4} \quad (6)$$

$$X_{tt} = \left(\frac{1-x}{x}\right)^{0.9}\left(\frac{\rho_v}{\rho_l}\right)^{0.5}\left(\frac{\mu_l}{\mu_v}\right)^{0.1}. \quad (7)$$

In order to predict the heat transfer coefficients for both pure and mixed refrigerants under the suppression of nucleate boiling, a certain form of $F(X_{tt})$ is needed. For this purpose, the empirically determined $F(X_{tt})$ by Chen [16] is chosen since it has been the most popular one. Chen's F function was originally given in a graphical form and later correlated by Cooper [17] as

$$F = 1 + 1.8\left(\frac{1}{X_{tt}}\right)^{0.82}. \quad (8)$$

A traditional way to check if nucleate boiling is suppressed is to see the dependence of the two-phase heat transfer coefficient on mass flow rate. Under the suppression of nucleate boiling, equation (5) with

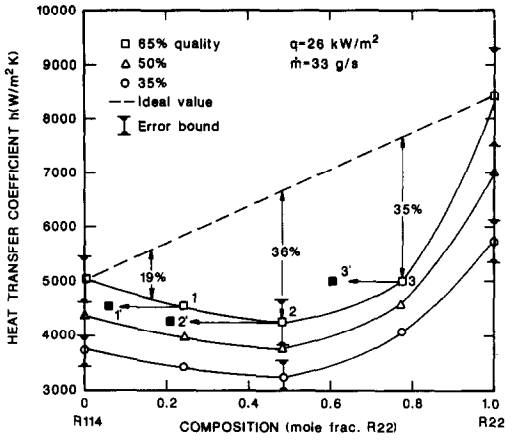

FIG. 5. Heat transfer coefficients of pure and mixed refrigerants of R22 and R114 in convective evaporation region as functions of composition and quality at $p_r = 0.08$.

equation (6) states that the two-phase heat transfer coefficient is proportional to the mass flow rate to the power 0.8

$$h_{tp} \propto \dot{m}^{0.8}. \tag{9}$$

The present data beyond transition qualities in Figs. 3 and 4 indeed follow the trend of equation (9) indicating that nucleate boiling is suppressed. The results obtained with R114 and mixtures at other compositions reveal a similar trend.

In 1979, Toral [18] showed that the complete suppression of nucleate boiling would not occur under common conditions in an annular flow boiling of organic fluids such as refrigerants due to a relatively low thermal conductivity. Ross *et al.* [6], however, observed the complete suppression of nucleate boiling with pure R152a at low pressures. At higher pressures, however, nucleate boiling was not suppressed. Conventional nucleation theory states the required wall superheat for nucleation of bubbles becomes greater as pressure decreases. Consequently, nucleate boiling is better suppressed at lower pressures with the same wall superheat. The present results obtained at relatively low pressures support the observation of Ross *et al.* [6].

3.2. *Heat transfer analysis in evaporation region*

Since the majority of the data for both pure and mixed refrigerants belongs to the convective evaporation region, the focus of the heat transfer analysis will be given to the data in this region.

3.2.1. *Pure fluids.* Figure 5 illustrates the typical heat transfer characteristics for pure and mixed refrigerants under the suppression of nucleate boiling as functions of quality and overall composition. It is observed that at qualities over 40% the heat transfer coefficients for pure R22 are usually 50–70% higher than those for pure R114. For instance, the heat transfer coefficients for pure R22 and R114 are 8400 and 5050 W m^{-2} °C^{-1}, respectively, for the condition of 26 kW m^{-2} and 33 g s^{-1} at 65% quality as shown in Fig. 5. Since quality is high and a full suppression of nucleate boiling is indicated, equations (5)–(7) apply for the heat transfer prediction in this region. For the same mass flux and a given diameter, equation (5) can be written as

$$h_{tp} \propto k_l^{0.6}(C_{pl}/\mu_l)^{0.4}(1-x)^{0.8}F(X_{tt}) = \phi F(X_{tt}) \tag{10}$$

where

$$\phi = k_l^{0.6}(C_{pl}/\mu_l)^{0.4}(1-x)^{0.8}.$$

Recently, Cooper [17] has shown that for pure fluids the property group in X_{tt} can be well correlated by using a reduced pressure, p_r. For water, Cooper suggested

$$\left(\frac{\rho_v}{\rho_l}\right)^{0.5}\left(\frac{\mu_l}{\mu_v}\right)^{0.1} = 0.37p_r^{0.37}. \tag{11}$$

By taking the same approach for refrigerants (R22, R114, R12, R152a), the property group in X_{tt} is correlated as

$$\left(\frac{\rho_v}{\rho_l}\right)^{0.5}\left(\frac{\mu_l}{\mu_v}\right)^{0.1} = 0.551p_r^{0.492}. \tag{12}$$

Equation (12) is applicable in the range of $0.06 < p_r < 0.7$ with a maximum deviation of 4%.

By using equation (12), X_{tt} for refrigerants can be written as

$$X_{tt} = 0.551\left(\frac{1-x}{x}\right)^{0.9} p_r^{0.492}. \tag{13}$$

For the same quality, equation (10) combined with equation (13) becomes a function only of liquid phase properties and a reduced pressure

$$h_{tp} \propto k_l^{0.6}(C_{pl}/\mu_l)^{0.4} fn(p_r). \tag{14}$$

Since the present study was undertaken at the same reduced pressure of 0.08, the two-phase heat transfer coefficient in equation (14) becomes a function only of the combination of three properties, namely, k_l, C_{pl},

and μ_l. When appropriate property values for the given condition, as listed in Table 1, are used in equation (14), the heat transfer coefficients for R22 are predicted to be 63% greater than those for pure R114 when nucleate boiling is suppressed, which is in excellent agreement with the experimentally determined values.

This analysis identifies the property group, $k_l^{0.6}(C_p/\mu)_l^{0.4}$, which is responsible for the two-phase heat transfer for pure fluids under the suppression of nucleate boiling and also suggests how to select a working fluid for good heat transfer by comparing the values of the property group in equation (14) for various pure fluids in conjunction with an appropriate F function.

3.2.2. *Mixtures.* Figure 5 illustrates that the heat transfer coefficients for mixtures are always lower than the values calculated by an ideal mixing rule (dashed line) for the same flow condition. For instance, at 65% quality, the deviation of heat transfer coefficients for mixtures from the ideal values are 19, 36, and 35% for the overall compositions of 0.23, 0.47, 0.77 of R22, respectively. Since data for mixtures also reveals the suppression of nucleate boiling, equation (10) again can be used for the prediction of heat transfer. As shown earlier, for pure components, $F(X_{tt})$ is a function only of a reduced pressure and quality. This, however, may not be true of mixtures because the property groups in X_{tt} and h_{tp} in equation (10) may reveal non-ideal characteristics due to mixing.

For mixtures in the two-phase region, as quality is increased, local liquid phase composition varies such that the liquid film at higher qualities is increasingly enriched in the less volatile component, R114 in this study. For instance, local liquid compositions for points 1, 2, and 3 in Fig. 5 are 0.08, 0.231, and 0.57 mole fraction R22 even though the overall compositions for those points are 0.23, 0.47, and 0.77, respectively. As a consequence of this local liquid phase composition shift, heat transfer coefficients for mixtures at high qualities would reflect more the liquid properties of the less volatile component than indicated by the overall composition value.

The calculation procedure for the two-phase heat transfer coefficient for mixtures in equation (10) is as follows; for the same reduced pressure, quality, and overall composition, the equilibrium liquid and vapor phase compositions, C_l and C_v, and corresponding equilibrium temperature, T_{eq}, are calculated by the CSD equation of state. Consequently, X_{tt}, $F(X_{tt})$ of Chen, and the property and quality combination in equation (10), ϕ, and finally $\phi F(X_{tt})$ are evaluated from the properties for pure components at the equilibrium temperature, T_{eq}, by the best available mixing rules at equilibrium liquid and vapor phase compositions (not at the overall composition).

Figure 6 shows the variations of $1/X_{tt}$, ϕ, and $\phi F(X_{tt})$ as a function of overall composition for various qualities at the same reduced pressure of 0.08. A reciprocal of the Martinelli parameter, $1/X_{tt}$, is shown to be constant at low qualities and varies a little bit at high qualities. The property and quality combination, ϕ in equation (10), gradually changes from 0 to 0.6 mole fraction of R22 and increases sharply from the overall composition 0.6–1. The dotted lines in Fig. 6(b) represent the ϕ curve which would be obtained if properties varied ideally.

The degradation of ϕ from the curve calculated by a linear mole fraction weighting of pure component values is composed of two portions. A portion (indicated as 'A' in Fig. 6) is caused by the equilibrium temperature variation due to mixing and the liquid phase composition shift at high qualities as explained earlier, which cannot be avoided for mixtures with different boiling points. A portion 'B', however, is due to the non-ideal variation of mixture properties, which would be absent if properties varied ideally. Portion 'B' is discussed in detail by Ross [19]. Another point to be noted is that portion 'A' is two to three times larger than portion 'B' implying that most of the degradation in ϕ and consequently in the heat transfer coefficient comes from the former cause.

Two-phase heat transfer coefficients, which would be predicted by equation (10), increase gradually in the range of 0–0.6 mole fraction R22 and show a sharp increase at compositions near R22 as shown in Fig. 6(c). This result clearly indicates that two-phase flow heat transfer coefficients for R22/R114 mixtures cannot be greater than the ideal values calculated by a linear mixing rule when boiling is fully suppressed. The maximum degradation of this property group for R22/R114 mixtures, approximately 20–27% from the ideal value, is shown to occur at the composition range of 0.4–0.8 mole fraction R22 as seen in Fig. 6(c).

This physical property variation associated with mixtures is responsible for the degradation of heat transfer coefficients from the ideal values up to 27%, which constitutes roughly 80% of the total degradation seen with R22/R114 mixtures as compared to the data shown in Fig. 5. The remaining 20%, which is less than 10% of the total heat transfer coefficient and not accounted for by the physical property variation, is believed to be from mass transfer resistance in evaporation with mixtures.

3.3. *Gradual change in composition near pure* R22

It is also shown in Fig. 5 that heat transfer coefficients with mixtures for the same conditions of heat and mass fluxes and quality are more or less the same over the composition range of 0.23–0.77 within 10% deviation. Furthermore, heat transfer coefficients at an overall composition of 0.77 appear to drop abruptly from the values for pure R22. These results raise the question about heat transfer coefficients being a function of mixture composition at all, except for 'near pure component mixtures'. In order to see how heat transfer coefficients vary at compositions close to a pure component, a series of tests were carried out for two sets of flow conditions

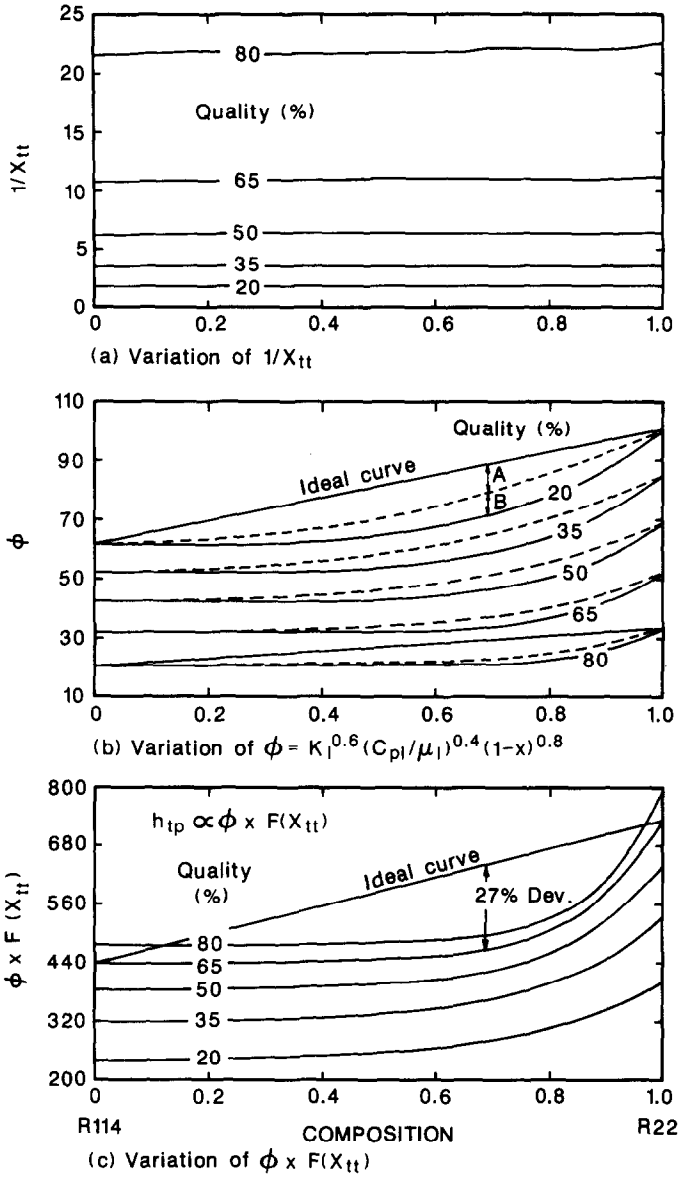

FIG. 6. Variations of $1/X_{tt}$, ϕ, and $\phi F(X_{tt})$ for various qualities as a function of overall composition at $p_r = 0.08$. (Units in Table 1 are used for the calculation.)

with the composition changing from 100% R22 to 85% R22/15% R114 in several steps. Figure 7 shows the results for $q = 17$ kW m^{-2} and $\dot{m} = 23$ g s^{-1} at different qualities. Tests at $q = 26$ kW m^{-2} and $\dot{m} = 23$ g s^{-1} also show a similar trend.

Heat transfer coefficients are seen to drop smoothly as R114 is added to R22. This result indicates that the heat transfer coefficients for mixtures are indeed a function of an overall composition and nothing abrupt happens as one adds a small amount of a second component to a pure refrigerant. Theoretical analysis presented above and shown in Fig. 6(c) supports this point and also explains where the steep gradient observed at compositions near R22 in Fig. 7 comes from. The fact that the h_{tp} vs composition curve is steeper near the R22 end may be due to the additive effects of adding R114, which has poorer heat transfer characteristics, as well as mixture property effects. Whereas at the R114 side, the effects oppose each other causing a less rapid degradation with a change in composition.

3.4. *Data analysis using dimensionless parameters*

The plot of the two-phase heat transfer multiplier, h_{tp}/h_{lo}, against a reciprocal of the Martinelli parameter, $1/X_{tt}$, is made in order to take into account the effects of various test conditions and physical property variations as suggested by Bergles *et al.* [20]. Figures 8 and 9 illustrate the results for pure and mixed refrigerants of R22 and R114. In these figures, h_{tp} is a measured heat transfer coefficient and h_{lo} and X_{tt} are given by equations (6) and (7). Mixture

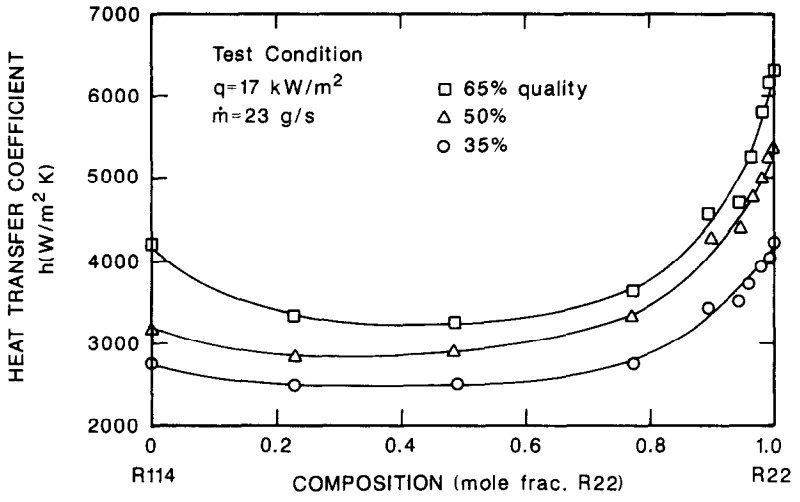

FIG. 7. Effect of gradual change in composition near R22 on heat transfer with mixtures at $p_r = 0.08$.

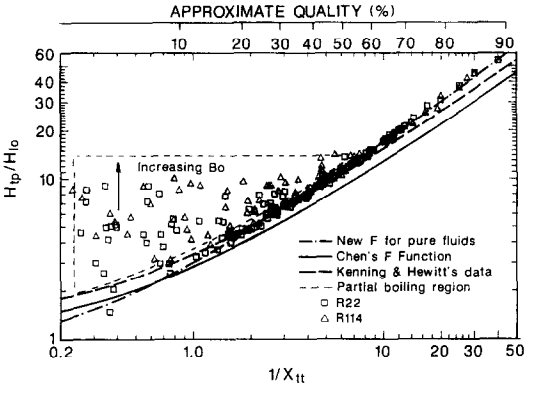

FIG. 8. Flow boiling heat transfer results for pure R22 and R114 at $p_r = 0.08$ using dimensionless parameters.

properties are evaluated at local equilibrium liquid and vapor phase compositions. Also shown are a new F factor approximating the present results for pure fluids, the F factor by Chen given in equation (8), and the curve fit for Kenning and Hewitt's water data [8], which were obtained under the suppression of nucleate boiling.

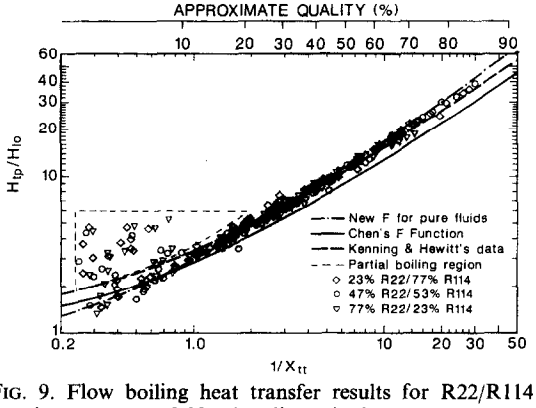

FIG. 9. Flow boiling heat transfer results for R22/R114 mixtures at $p_r = 0.08$ using dimensionless parameters.

3.4.1. *Pure fluids.* As seen in Fig. 8, for pure refrigerants heat transfer coefficients are scattered at low qualities indicated by the area enclosed by the dashed line (partial boiling regime) and they fall into a single line outside the area. For a given condition, nucleate boiling is not fully suppressed until a transition point (or quality) is reached as explained earlier. In the partial boiling regime, heat transfer coefficients are a function of both heat flux and mass flow rate. This can be seen very well by introducing another dimensionless quantity called boiling number defined as

$$Bo = \frac{q}{(Gh_{fg})}. \tag{15}$$

Bo can be interpreted as the ratio of the mass flux of vapor generated on the heated surface to the total mass flux parallel to the heated surface. Shah [21] showed that heat transfer coefficients in the partial boiling regime are a strong function of Bo. The higher the Bo, the larger the heat transfer coefficients. Outside the partial boiling regime, all data fall into a single line within experimental error, showing only the dependence of heat transfer coefficients on quality or $1/X_{tt}$. For high mass flow rate and low heat flux (small Bo), heat flux dependence quickly disappears at very low qualities. For low mass flow rate and high heat flux (large Bo), the dependence of heat transfer coefficients on heat flux persists to high qualities and finally boiling is suppressed beyond a transition point.

As listed in Table 1, heat of evaporation of R114 is smaller than that of R22, which results in a higher Bo for R114 than for R22 under the same mass flow rate and heat flux. This is the reason why data for R114 in the partial boiling regime extends to high quality ranges. In this regard, further work is needed to predict the point of suppression of nucleate boiling under

a given flow condition with various working fluids and also to develop a correlation in both partial and fully suppressed boiling regimes.

Figure 8 also shows that the F factor by Chen severely underpredicts the new F factor for pure components by 20–30% with the larger deviation observed at higher qualities. This indicates that the F factor in Chen's equation is not relevant for pure refrigerants, as reported by previous investigators [10, 15]. It may be due to the fact the F factor by Chen was originally obtained from steam–water data at relatively low qualities.

This is supported by the recent data by Kenning and Hewitt [8]. They obtained heat transfer coefficients for steam–water at 160 and 390 kPa in a 9.6 mm bore tube up to 65% quality. When nucleate boiling is suppressed, their data fall close to a single line, lying roughly 20% above the F factor by Chen as shown in Fig. 8. They attributed the large discrepancy among many experimental data in the literature to the inaccuracy of the local pressure and saturation temperature measurements. The present data for pure refrigerants and data for steam–water by Kenning and Hewitt under the suppression of nucleate boiling agree very well up to 65% quality, which is the maximum quality obtained by Kenning and Hewitt. This implies that this new F function may be used for the heat transfer prediction under this condition for other fluids since water and refrigerants are very different fluids.

3.4.2. *Mixtures.* Figure 9 shows that for mixtures the scatter of data due to nucleate boiling is limited to qualities below 15% and beyond this quality all data lie on a single line. Ross *et al.* [6] observed that nucleate boiling was very well suppressed for R13B1/R152a mixtures. This can be explained as follows; in bubble growth dynamics, it is usually assumed [22] that a temperature gradient exists between the superheated solid surface and liquid/vapor interface and the heat required for vapor generation is supplied by the heat conducted across the temperature gradient. Thus, for pure fluids, the bubble growth rate is limited by the rate of heat conduction.

In addition to this, another limitation exists during the bubble growth of mixtures. The difference in volatilities of the two components causes a stripping of the more volatile component near the bubble interface. Thus, the mole fraction of the more volatile component of the liquid at the interface is smaller than that in the bulk, resulting in an increase in saturation temperature at the interface. This phenomenon, consequently, reduces the available effective driving temperature potential for the supply of heat for bubble generation. This effect is found to be present for any mixture except for the special case of an azeotrope which has no preferential stripping to cause a composition shift at the interface [22].

Scriven [23] solved analytically the growth rate of an isolated spherical bubble located in quiescent, uniformly superheated liquid. The results showed a reduction in bubble growth rate for a mixture over that of an equivalent pure fluid due to mass transfer resistance explained above. Hui and Thome [24] measured the boiling site densities for ethanol–water and ethanol–benzene mixtures and observed a decrease in boiling site densities for mixtures. These effects would lower the contribution by nucleate boiling on flow boiling heat transfer of mixed refrigerants and hence the suppression of nucleate boiling with mixtures would occur easily at lower qualities as indicated in Fig. 9.

Figure 9 also illustrates that data for mixtures under the suppression of nucleate boiling lie up to 10% below the new F factor for pure refrigerants. Since the physical property variations associated with mixtures are already taken into consideration in Fig. 9, the most probable source of this deviation is the unaccounted portion in heat transfer degradation due to mass transfer resistance, roughly 10% of the total heat transfer coefficient as explained in Figs. 5 and 6. This suggests that mass transfer resistance, known as the principal cause for the substantial reduction in nucleate pool boiling heat transfer coefficients for mixtures [7, 22], is small for flow boiling heat transfer under the suppression of nucleate boiling.

This supports the findings of Berntsson *et al.* [25] and Shock [26]. Berntsson *et al.* [25] measured the evaporative heat transfer coefficients for non-azeotropic mixtures of R12 and R114 in a falling film heat exchanger and concluded that the additional mass transfer resistance due to mixing is small or negligible in a falling film at surface evaporation conditions (i.e. no bubbles formed on the surface). Shock [26] studied analytically the evaporation of binary mixtures in annular flow and showed that heat transfer through the liquid film is not significantly affected by the mass transfer resistance occurring within it.

In this regard, further experiments are needed with an azeotropic mixture to eliminate the effect due to mass transfer resistance on heat transfer since this mixture has the same liquid and vapor phase compositions in the two-phase region at an azeotrope. Except for an azeotrope, however, mixtures at other compositions would behave in the similar fashion as non-azeotropic mixtures. The results with this azeotropic mixture then would reveal only other mixture effects such as the property variation on heat transfer at an azeotrope and the effect due to mass transfer resistance (i.e. reduction in heat transfer coefficient) would be revealed clearly at other compositions.

3.5. *Circumferential variation of temperature, composition and heat transfer coefficient*

Figure 10 illustrates wall temperature profile vs quality for pure and mixed refrigerants for the same flow condition. Since quality is over 20%, an annular flow pattern is observed. For pure components, the temperature at the bottom is higher than the one at the top by 0.1–0.3°C. For mixtures, however, the

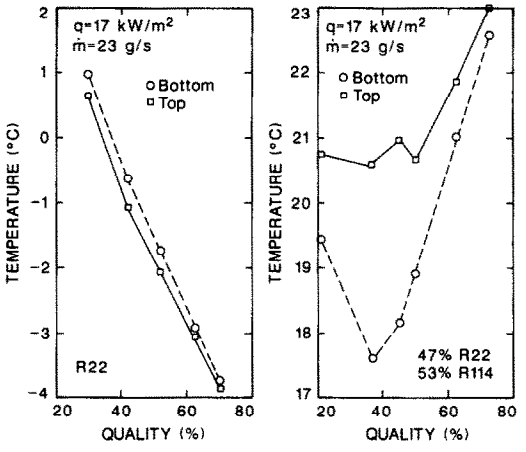

FIG. 10. Circumferential variation of wall temperatures for pure and mixed refrigerants of R22 and R114 at $p_r = 0.08$.

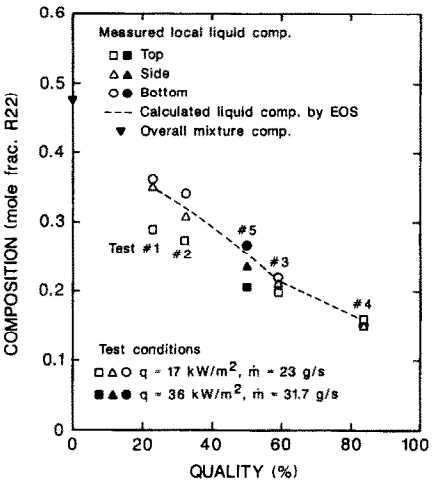

FIG. 12. Comparison of the measured and calculated liquid compositions.

temperature at the bottom is lower than the one at the top by as much as 4°C at low qualities with smaller differences at higher qualities. Figure 11 shows the heat transfer coefficients calculated by the method presented above, equation (1), for pure and mixed refrigerants for the same flow condition. For mixtures, the coefficients at the top are severely degraded as compared to those at the bottom.

Local liquid film composition measurements were conducted to explore this unique behavior of mixtures for two sets of flow conditions at several qualities. Figure 12 shows the measured overall and local liquid compositions and the average equilibrium liquid compositions calculated by the CSD equation of state based on measured pressures, specific enthalpies, and overall compositions. Measured local liquid compositions at the top are always smaller than the ones at the bottom except for test 4. For test 4, quality at the sampling port was 82% and local dryout may have happened at the top so that vapor was drawn with the sample.

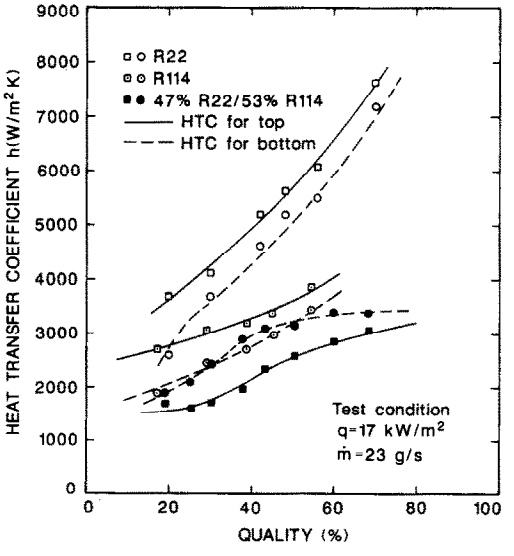

FIG. 11. Circumferential variation of heat transfer coefficients for pure and mixed refrigerants of R22 and R114 at $p_r = 0.08$.

Calculated equilibrium compositions by the CSD equation of state always fall in between the measured values for the top and bottom and are close to the ones for the side. The present results clearly reveal a circumferential composition variation as large as 0.07 mole fraction at relatively low qualities with smaller composition differences at higher qualities. This indicates that mixtures are not fully mixed circumferentially. The top is richer in the less volatile component, R114, and the bottom is richer in the more volatile component, R22. This result confirms the conjecture by Ross *et al.* [6].

The cause for the circumferential variation of composition may be explained as follows; since the heat flux is uniform, the rate of vapor generation will also be uniform. But the liquid film at the top is thinner due to gravity and thus evaporating vapor, enriched in the more volatile component, at a constant rate will cause the remaining liquid at the top to shift in composition towards the less volatile component more rapidly than at the bottom. This is due simply to the requirements of a mass and species balance. The existence of significant circumferential composition variation implies that there is relatively little top-to-bottom mixing. At higher qualities, the composition of the liquid film is seen to be nearly uniform circumferentially. This may be due to the reduced influence of gravity with the thinner liquid film and higher vapor velocity at high qualities or perhaps to a more rapid equilibration between the liquid and vapor.

As a result of this composition variation, the local equilibrium temperatures are different circumferentially. This result explains why heat transfer coefficients at the bottom are better than the ones at the top in an annular flow regime for mixtures. In calculating heat transfer coefficients for mixtures, equation (1) has been used in refs. [5, 6], and so far

Table 2. Comparison of the measured liquid compositions and calculated ones by equation of state and heat transfer coefficients calculated by two methods

Test no.	Location	Measured local liquid composition C_l	Local equilibrium fluid temperature based on C_l T_{eql} (°C)	Calculated average fluid temperature by EOS T_{eqa} (°C)	Measured wall temperature T_w (°C)	*HTC* based on T_{eql} h_{eql} (W m^{-2} K^{-1})	*HTC* based on T_{eqa} h_{eqa} (W m^{-2} K^{-1})
1	t	0.29	10.04		18.8	1946	1393
	s	0.35	6.49		16.57	1697	1708
	b	0.36	5.95		16.81	1575	1667
	av			6.55		1728	1619
2	t	0.273	11.72		17.4	3019	1942
	s	0.309	9.4		15.0	3062	2681
	b	0.341	7.52		13.8	2740	2580
	av			8.56		2971	2649
3	t	0.2	16.84		21.41	3761	2765
	s	0.21	16.0		20.68	3673	3138
	b	0.218	15.38		20.05	3680	3546
	av			15.20		3697	3147
4	t	0.162	18.49		23.66	3280	3079
	s	0.151	19.51		23.46	4292	3200
	b	0.152	19.41		23.19	4485	3368
	av			18.15		4087	3212
5	t	0.206	17.44		25.51	4423	2982
	s	0.235	15.19		23.52	4284	3581
	b	0.266	13.0		21.11	4401	4714
	av			13.54		4424	3714

in this study with the assumptions that both phases are in equilibrium and that the composition of each phase is uniform over a given cross-section of the heated tube. The results from the local liquid composition measurements, however, indicate that at least the latter assumption is not valid. Actual local heat transfer coefficients for mixtures may be obtained by using local equilibrium temperatures, T_{eql}, which are calculated by the CSD equation of state given a measured pressure and a measured liquid composition.

Table 2 lists heat transfer coefficients calculated by two sets of fluid temperatures: T_{eqa} and T_{eql}. When the local equilibrium fluid temperature, T_{eql}, is used in calculating the heat transfer coefficient, the heat transfer coefficients at the top are actually greater than the ones at the bottom even with mixtures. This is the behavior observed with pure components in an annular flow regime and is reasonable since the hydrodynamics of mixtures and pure components should be similar in horizontal geometry. Another fact to be noted is that the average heat transfer coefficients based on the local equilibrium fluid temperatures show a 10–20% increase as compared to those based on the average equilibrium fluid temperatures. This indicates that a portion of the degradation in heat transfer with mixtures may be an artifact of how the heat transfer coefficient is calculated.

Since the measurement of local liquid compositions for each thermocouple location would require a huge effort, the conventional approach to calculate the heat transfer coefficients for mixtures, equation (1), based on an average equilibrium fluid temperature, T_{eqa}, has been preferred throughout this study. Also this approach would be the one most likely to be used in heat exchanger design. In order to reduce the effect of circumferential composition variation and to improve the heat transfer characteristics for mixtures, swirl generators or spiral flow generators may be inserted in the heated tube.

4. CONCLUSIONS

Based on the present experimental study of horizontal flow boiling heat transfer with non-azeotropic mixtures of R22 and R114, the following conclusions can be reached.

(1) A full suppression of nucleate boiling has been observed for both pure and mixed refrigerants at qualities above 10–30% depending upon the test conditions. Flow boiling heat transfer coefficients for R22/R114 mixtures in the convective evaporation region are always lower than the values calculated by an ideal mixing rule with two pure component coefficients. The degradation of heat transfer coefficients for mixtures from the ideal values was up to 36% depending on the overall composition.

(2) Under the suppression of nucleate boiling, the physical property variation associated with mixtures is responsible for the degradation of heat transfer coefficients from the ideal values up to 27%, which accounts for up to 80% of the observed heat transfer degradation seen with mixtures. A simple method is suggested on how to select a working fluid for better heat transfer by considering a relevant property group with an appropriate F function.

(3) The effect due to the additional mass transfer resistance on heat transfer coefficients for R22/R114 mixtures seems small, less than 10% of the total heat transfer coefficient, under the suppression of nucleate

boiling. A further study with azeotropic mixtures is suggested to clarify the role of mass transfer resistance on heat transfer coefficients for mixtures.

(4) Experiments with a gradual change in composition near R22 revealed that heat transfer coefficients for mixtures at compositions close to pure R22 change smoothly and also they are a strong function of overall composition over the range of 0.85–1. The steep gradient near the R22 side in the h_{tp} vs composition diagram is caused by the physical property variation.

(5) A circumferential variation in wall temperature and heat transfer coefficient for R22/R114 mixtures opposite that of pure components has been observed, generalizing the observation of Ross for a R13B1/R152a mixture. A circumferential variation in liquid film composition of up to 0.07 mole fraction was measured. The resulting variation in local saturation temperature explains the observed circumferential wall temperature variation.

Acknowledgements—This work was funded by the Electric Power Research Institute (Project No. RP8406-2 under the supervision of Dr Jong Kim, Project manager) and the National Bureau of Standards and was carried out in the laboratories of NBS. The authors would like to acknowledge the many helpful discussions with H. Ross and his contribution in the design of the current experimental apparatus.

REFERENCES

1. W. Mulroy, M. Kauffeld, M. McLinden and D. Didion, An evaluation of two refrigerant mixtures in a breadboard air conditioner, International Institute of Refrigeration Conference, Purdue University, July (1988).
2. C. P. Arora, Power savings in refrigerating machines using mixed refrigerants, *Proc. XII Int. Congress Refrigeration*, Madrid, Vol. 2, pp. 397–409 (1967).
3. W. Mulroy and D. Didion, The performance of a conventional residential sized heat pump operating with a nonazeotropic binary refrigerant mixture, NBSIR 86-3422, NBS, Gaithersburg, MD 20899 (1986).
4. L. C. Singal, C. P. Sharma and H. K. Varma, Experimental heat transfer coefficient for binary refrigerant mixtures of R13 and R12, *ASHRAE Trans.* No. 2747, 175–188 (1983).
5. R. Radermacher, H. Ross and D. Didion, Experimental determination of forced convective evaporative heat transfer coefficients for nonazeotropic refrigerant mixtures, ASME National Heat Transfer Conference, ASME 83-WA/HT54 (1983).
6. H. Ross, R. Radermacher, M. di Marzo and D. Didion, Horizontal flow boiling of pure and mixed refrigerants, *Int. J. Heat Mass Transfer* **30,** 979–992 (1987).
7. K. Stephan, Heat transfer in boiling mixtures, *Proc. 7th Int. Heat Transfer Conf.*, Munich, Paper RK14 (1982).
8. D. Kenning and G. Hewitt, Boiling heat transfer in the annular flow regime, *Proc. 8th Int. Heat Transfer Conf.*, San Francisco, pp. 2185–2190 (1986).
9. G. Morrison and M. O. McLinden, Application of a hard sphere equation of state to refrigerants and refrigerant mixtures, NBS Technical Note 1226, NBS, Gaithersburg, MD 20899 (1986).
10. J. B. Chaddock and A. P. Mathur, *Heat Transfer to Oil–Refrigerant Mixtures Evaporating in Tubes, Multiphase Transport—Fundamentals, Reactor Safety, Applications*, Vol. 2, pp. 861–884. Hemisphere, Washington, DC (1967).
11. H. P. Soumerai, Thermodynamic generalization of heat transfer and fluid flow data, *ASHRAE Trans.* No. 4, 776–790 (1986).
12. M. G. Cooper, Heat flow rates in saturated nucleate pool boiling—a wide ranging examination using reduced properties. In *Advances in Heat Transfer*, Vol. 16. Academic Press, New York (1984).
13. Private communication with Dr A. Johns, National Engineering Laboratory, East Kilbride, Scotland.
14. R. C. Reid, J. M. Prausnitz and T. K. Sherwood, *The Properties of Gases and Liquids*. McGraw-Hill, New York (1977).
15. J. B. Chaddock and J. A. Noerager, Evaporation of refrigerant 12 in a horizontal tube with constant wall heat flux, *ASHRAE Trans.* **72,** 90–103 (1966).
16. J. C. Chen, Correlation for boiling heat transfer to saturated fluids in convective flow, *Ind. Engng Chem. Proc. Des. Dev.* **5,** 322–329 (1966).
17. Private discussion with M. G. Cooper at Oxford University.
18. H. Toral, Flow boiling heat transfer in mixtures, Ph.D. Thesis, University of Oxford, Oxford (1979).
19. H. Ross, An investigation of horizontal flow boiling of pure and mixed refrigerants, Ph.D. Thesis, University of Maryland, College Park (1985).
20. A. E. Bergles, J. G. Collier, J. M. Delhaye, G. F. Hewitt and F. Mayinger, *Two-phase Flow and Heat Transfer in the Power and Process Industries*. Hemisphere, Washington, DC (1981).
21. M. M. Shah, A new correlation for heat transfer during boiling flow through pipes, *ASHRAE Trans.* **82,** 66–86 (1976).
22. R. A. Shock, *Boiling in Multicomponent Fluids, Multiphase Science and Technology* (Edited by G. F. Hewitt, J. M. Delhaye and N. Zuber), Vol. 1. Hemisphere, Washington, DC (1982).
23. L. D. Scriven, On the dynamics of phase growth, *Chem. Engng Sci.* **10,** 1–13 (1959).
24. T. O. Hui and J. R. Thome, A study of binary mixture boiling: boiling site density and subcooled heat transfer, *Int. J. Heat Mass Transfer* **28,** 919–928 (1985).
25. T. Berntsson, K. M. Berntsson and H. Panholzer, Heat transfer of nonazeotropic mixtures in a falling film evaporator, *ASHRAE Trans.* **91,** 1337–1350 (1985).
26. R. A. Shock, Evaporation of binary mixtures in upward annular flow, *Int. J. Multiphase Flow* **2,** 411–433 (1976).

EXPERIENCES SUR LE TRANSFERT THERMIQUE PAR EBULLITION POUR UN ECOULEMENT HORIZONTAL DE MELANGE R22/R114

Résumé—On décrit une étude expérimentale sur le transfert thermique par ébullition dans un écoulement horizontal de R22 et R114 purs et de leurs mélanges, sous des conditions de flux de chaleur uniforme. Plus de 1200 valeurs du coefficient local de transfert sont obtenues pour l'écoulement annulaire à une pression réduite de 0,08. Les domaines explorés sont pour le flux thermique 10–45 kW m^{-2} et pour le débit 16–46 g s^{-1}. Les résultats montrent une suppression complète de l'ébullition nucléée pour les refrigérants purs et mélangés au delà des qualités de transition et la majorité des cas appartient à la région d'évaporation convective. Les coefficients de transfert thermique des mélanges, dans cette région, sont jusqu'à 36% plus faibles que les valeurs idéales dans les mêmes conditions. Des variations non idéales dans les propriétés physiques comptent pour 80% dans la dégradation du transfert thermique observée avec les mélanges et les autres 20% (moins de 10% du coefficient de transfert thermique) semble être causé par la résistance au transfert de masse dans cette région. Une variation de composition jusqu'à 0,07 en fraction molaire dans le film annulaire liquide a été mesurée entre le sommet et la base du tube, ce qui cause une variation circonférentielle de température pariétale avec les mélanges.

EXPERIMENTELLE UNTERSUCHUNG DES WÄRMEÜBERGANGS BEIM HORIZONTALEN STRÖMUNGSSIEDEN EINES R22/R114-GEMISCHES

Zusammenfassung—Die Arbeit befaßt sich mit der experimentellen Untersuchung des Wärmeübergangs beim horizontalen Strömungssieden von reinem R22 und R114 sowie auch Gemischen der beiden bei gleichförmiger Wärmestromdichten-Verteilung. Im Ringströmungs-Gebiet wurden bei einem normierten Druck von 0,08 mehr als 1200 örtliche Wärmeübergangskoeffizienten bestimmt. Der Bereich der Wärmestromdichte war 10–45 kW m^{-2}, der des Massestroms 16–46 g s^{-1}. Für die reinen Kältemittel und ihre Gemische deuten die Ergebnisse auf eine vollständige Unterdrückung des Blasensiedens jenseits der Übergangs-Dampfgehalte hin—die Mehrheit der Meßwerte liegt im konvektiven Siedebereich. Die Wärmeübergangskoeffizienten der Gemische in diesem Gebiet sind bis zu 36% kleiner als die idealen Werte bei gleichen Strömungsbedingungen. Nicht-ideale Änderungen der Stoffwerte sind für 80% der bei den Gemischen beobachteten Verringerungen der Wärmeübergangskoeffizienten verantwortlich—die restlichen 20% (weniger als 10% der Wärmeübergangskoeffizienten) werden dem Stofftransport-Widerstand zugeschrieben. Im ringförmigen Flüssigkeitsfilm wurden bei den Gemischen Änderungen im Molenbruch von bis zu 0,07 (zwischen oben und unten im Rohr) gemessen, was entsprechende Änderungen der Wandtemperaturen in Umfangsrichtung verursacht.

ЭКСПЕРИМЕНТАЛЬНОЕ ИССЛЕДОВАНИЕ ТЕПЛОПЕРЕНОСА ПРИ ГОРИЗОНТАЛЬНОМ ТЕЧЕНИИ КИПЯЩЕЙ СМЕСИ ФРЕОНОВ 22 И 114

Аннотация—Представлено экспериментальное исследование теплопереноса при горизонтальном течении кипящих чистых фреонов 22 и 114 и их смесей в условиях равномерного подвода тепла. Получено более чем 1200 локальных значений коэффициента теплопереноса для кольцевого течения при понижении давления до 0,08. Тепловой поток и расход жидкости исследовались соответственно в диапазонах 10–45 кВ $м^{-2}$ и 16–46 г $с^{-1}$. Результаты свидетельствуют о полном подавлении пузырькового кипения в случаях чистых фреонов и их смесей. Большая часть полученных данных относится к области конвективного испарения. Коэффициенты теплопереноса смесей в этой области на 36% ниже идеальных значений при тех же условиях течения. Неидеалные изменения физических свойств в 80% случаев вызывают ухудшение теплопереноса в смесях, а в остальных 20% вызваны, очевидно, сопротивлением массопереносу в этой области. Измерено изменение состава до 0,07 мольных долей в кольцевой пленке жидкости между верхней и нижней частями трубы, которое вызывает соответствующее изменение температуры стенок по периметру трубы.